Earthquake Engineering, Tenth World Conference © 1992 Balkema, Rotterdam. ISBN 90 5410 060 5

Study on soil properties of ground surface layers and characteristics of incident SH waves into sublayer

M. Ichikawa, T. Nishide & S. Sakai
Technical Research Institute of Hazama Corporation, Tsukuba, Japan

ABSTRACT: Soil properties of ground surface layers and characteristics of incident SH waves penetrating into the sublayer are presented. This is based on earthquake ground motion records and the inverse analysis method is used for the estimation of optimum soil parameters. In addition, the multiple regression technique is used for spectral characteristics of incident SH waves estimated from both the soil parameters and observed motions. The results show that estimated damping factors of soil deposits are dependent on frequency and the spectral characteristics of estimated incident SH waves are clearly different from the observed motions. In particular, the difference is greater in the vicinity of the predominant period of the ground surface layers.

1 INTRODUCTION

Amplification characteristics of earthquake motions in ground surface layers are one of the most important factors in the evaluation of earthquake motions at the ground surface. It appears that earthquake ground motions of short period are greatly influenced by subsurface structures. To discuss the amplification characteristics, the soil properties are very significant. Indications are that (modal) damping factors of soil deposits decrease in higher frequencies (modes), based on observed earthquake records (Yokota,1977; Kawamura,1977) and shaking table tests (Kitazawa et al.,1988).

The grasp of characteristics of incident waves penetrating into the sublayer is basically very important as well, because the amplification characteristics are different at each site while the characteristics of incident waves are generally discussed for a wider area. Incident waves, however, cannot be obtained directly from underground observation of earthquake motions because earthquake records contain the influence of the ground surface layers.

In this paper, soil properties of ground surface layers as well as spectral characteristics of incident SH waves penetrating into the sublayer are separated and discussed, based on earthquake records observed simultaneously at both surface and underground. The incident SH waves are also compared with observed underground motions.

2 OUTLINE OF OBSERVATIONS AND EARTHQUAKES

2.1 Observation sites

For the purpose of this study, earthquake ground motion records at two sites in Japan were analyzed. One is from the Technical Research Institute of Hazama Corporation (HAZM) in the Kwanto area for studying the degree of variation due to earthquakes. The soil profile is shown in Fig.1. The locations of seismometers for this study were 1.5 m deep (No.4, 'surface') and 46.8 m deep (No.1, 'underground').

The other consists of seven observatories utilizing the Dense Strong Motion Earthquake Seismometer Array in the Sendai area (MIYA, NAKA, TAMA, TSUT, OKIN, TRMA, SHIR; Kitagawa et al.,1988) used to study the degree of variable results among the observatories. The location of each observatory is shown in Fig.2, and the soil profiles are shown in Fig.3 (the rest can be seen in the paper by Kitagawa et al.,1988). The locations of

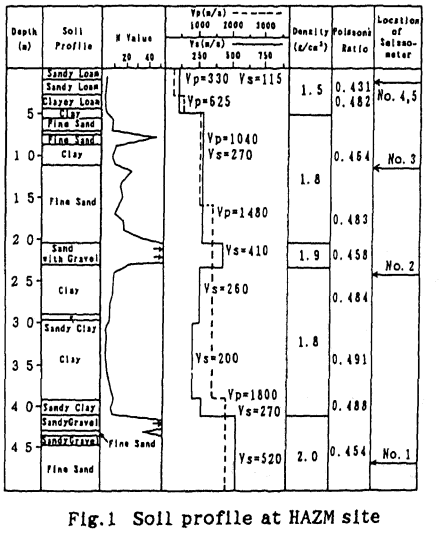

Fig.1 Soil profile at HAZM site

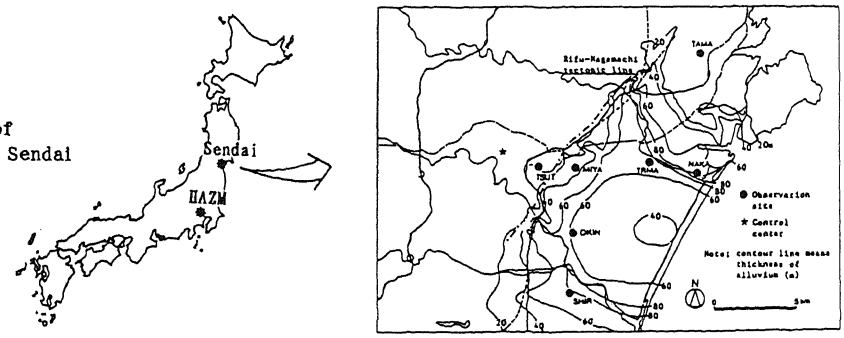

Fig.2 Location of observatories in Sendai and HAZM site

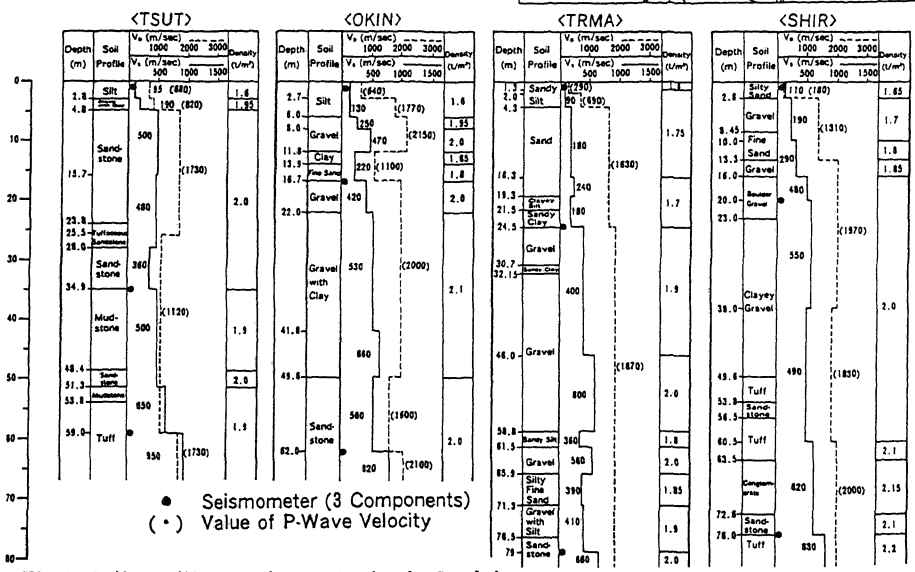

Fig.3 Soil profiles at observatories in Sendai

seismometers for this study were almost 1.5 m deep ('surface') and in a more shallow layer with a shear wave velocity (Vs) of more than 400 m/sec of the two ('underground').

2.2 Earthquakes

For the HAZM site, we analyzed 22 earthquake records which have an acceleration of more than 1 cm/sec^2 (for the maximum value of corrected transverse component; described later) underground, considering the S/N ratio of the earthquake records. The list of earthquakes is shown in Table 1. Magnitudes of these earthquakes were 4.5 ~ 6.8, and epicentral distances were 25 ~ 458 km.

For the Sendai site, we analyzed 12 earthquakes with magnitudes of 4.1 ~ 7.1 and epicentral distances of about 20 ~ 280 km, as shown in Table 2. These earthquakes were mostly observed in the east off Fukushima Pref. and in the vicinity.

3 PROCESSING OF OBSERVED MOTIONS

First of all, we corrected the observed

Table 1 List of earthquakes at HAZM site

No.	Origin Time Yea. Mon. Day. Hou. Min.	Epicenter	M	H (km)	Δ (km)	JMA Seis. Intensity TOKYO	JMA Seis. Intensity KUMAGAYA
1	'87. 4. 7. 9.41	E OFF FUKUSHIMA PREF.	6.6	44	255	IV	III
2	'87. 4.10.20. 0	SW IBARAKI PREF.	4.9	61	35	III	IV
3	'87. 4.17. 4.23	E OFF FUKUSHIMA PREF.	5.1	45	322	III	I
4	'87. 4.17.16.34	NORTHERN CHIBA PREF.	5.1	77	50	II	II
5	'87. 4.23. 5.13	E OFF FUKUSHIMA PREF.	6.5	47	224	III	II
6	'87. 6.30.18.17	SW IBARAKI PREF.	4.9	57	54	III	II
7	'87. 7.12.13.31	SW IBARAKI PREF.	4.6	57	49	II	III
8	'87. 7.16.14.48	FAR S OFF TOKAI DISTRICT	6.3	325	332	III	II
9	'87.10.16. 3.41	EASTERN YAMANASHI PREF.	4.8	32	60	II	II
10	'87.12.17.11. 8	KUJUKURI COAST BOSO PEN.	6.7	58	98	IV	IV
11	'88. 1.30. 6.19	E OFF IBARAKI PREF.	4.9	62	140	I	I
12	'88. 3.18. 5.34	TOKYO PREF.	6.0	96	25	III	IV
13	'88. 8.12.14.15	SOUTHERN BOSO PENINSULA	5.3	69	91	IV	II
14	'88. 9. 5. 0.49	EASTERN YAMANASHI PREF.	5.6	30	72	III	II
15	'88. 9.16. 3.19	SW IBARAKI PREF.	4.5	61	53	I	II
16	'88. 9.29.17.24	WESTERN SAITAMA PREF.	5.0	13	39	III	III
17	'88.10.28.15.14	SE OFF BOSO PENINSULA	5.1	76	104	II	II
18	'89. 2.19.21.27	SW IBARAKI PREF.	5.6	55	30	IV	III
19	'89. 3. 6.23.40	NORTHERN CHIBA PREF.	6.0	56	103	III	II
20	'89. 3.11.16.12	SOUTHERN IBARAKI PREF.	4.9	45	87	II	II
21	'89. 5. 9. 2.51	SW IBARAKI PREF.	4.7	72	56	–	II
22	'89. 6.17. 8.43	NEAR TORISHIMA ISLAND	6.8	385	458	III	II

Table 2 List of earthquakes in Sendai

EQ No.	Origin Time Yea. Mon. Day. Hou. Min.	Epicenter	M	H (Km)	Δ^{*1} (Km)	Intens. (Sendai)	Acc^{*1} (cm/sec^2)
8719	1987 4/ 7 9:41	E OFF FUKUSHIMA PREF.	6.6	44	130	IV	100.1
8721	1987 4/17 4:23	E OFF FUKUSHIMA PREF.	6.1	45	148	III	29.0
8724	1987 4/23 5:13	E OFF FUKUSHIMA PREF.	6.5	47	140	III	86.4
8739	1987 9/24 13:55	E OFF IBARAKI PREF.	5.8	41	183	III	24.1
8740	1987 10/ 4 19:27	E OFF FUKUSHIMA PREF.	5.8	42	124	III	54.0
8812	1988 10/19 9:09	E OFF FUKUSHIMA PREF.	5.8	32	154	II	20.4
8902	1989 2/ 4 19:57	E OFF FUKUSHIMA PREF.	5.4	61	108	II	-
8904	1989 2/15 13:53	E OFF MIYAGI PREF.	4.4	53	66	II	11.1
8911	1989 4/28 0:27	E OFF FUKUSHIMA PREF.	4.9	52	95	III	20.4
8915	1989 6/24 5:00	SOUTHERN MIYAGI PREF.	4.1	14	16	III	25.4
8925	1989 10/29 14:26	FAR E OFF SANRIKU	6.5	0	276	II	7.9
8926	1989 11/ 2 3:26	FAR E OFF SANRIKU	7.1	0	251	III	16.1

*) Values at the Surface of NAKA observatory (Acc : corrected TR Component)

accelerograms (i.e., base-line correction before F.F.T. band-pass filtering ; 0.1 ~ 10.0 Hz), and then calculated transverse (TR) components from two horizontal components of corrected accelerograms.

Finally we picked up only the main parts (about ten seconds) of the TR components, which can be regarded as observed SH waves, referring to the accelerograms themselves, the results of non-stationary spectrum analysis and particle motion orbits, shown in Fig.4 (a) ~ (c), respectively. We used the observed SH waves for sequent analysis.

4 PROCEDURE OF ANALYSIS AND RESULTS

The schematic diagram of the analytical model is shown in Fig.5. We first estimated optimum soil properties (Vs,h) of the ground surface layers from the observed SH waves, and then we calculated incident SH waves penetrating into the sublayer on a theoretical basis. The procedure of analysis and results are as follows.

4.1 Optimization technique

We regarded the Fourier spectrum ratio (surface/underground) of the observed SH waves as the transfer function in the case of seismic SH waves propagated obliquely through horizontally layered subsoil, and estimated the structure of the ground surface layers using the Simplex method, a kind of inverse analyses (Sakai et al.,1989). The Fourier spectrum ratios, which were target spectra for the optimization, were calculated after smoothing the Fourier spectra of the SH waves observed at the surface and underground by the Parzen window with a width of 0.2 Hz.

For optimization, the soil damping model of each layer was assumed to be dependent on frequency and may be written as

$$h_i = h_{1i} \times (f / f_1)^{\alpha_i} \qquad (1)$$

where f is frequency and f_1 is the predominant frequency of the ground surface layers. h_i and h_{1i} are soil damping factors at i layer corresponding to f and f_1, respectively. α_i is a parameter standing for dependence of soil damping factors on frequency.

The flow of optimization is shown in Fig.6. We actually repeated the optimization twice to be precise. We started the optimization with the shear wave velocity obtained from the results of the in-situ velocity measurement and uniform damping factor of 5 % at the predominant frequency for each layer. We judged the convergence of spectral matching in the optimization from the coefficient of variation at each trial.

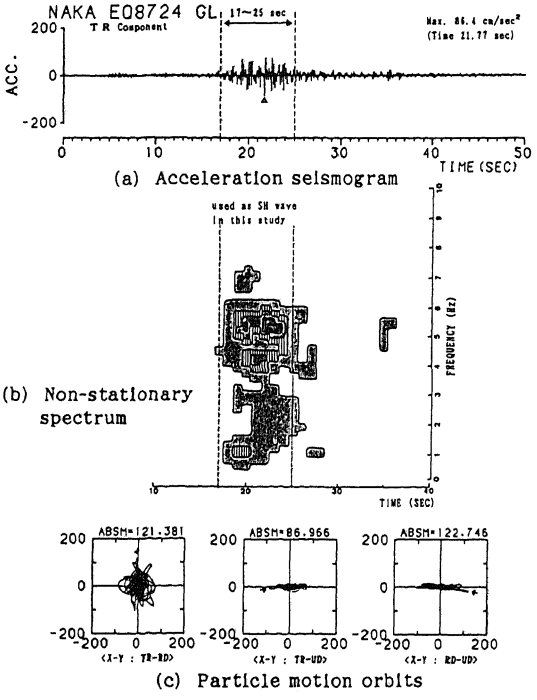

Fig.4 Pick-up of SH wave for EQ8724 earthquake at NAKA observatory in Sendai

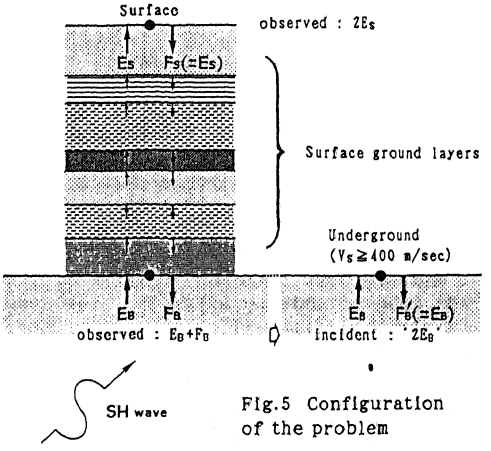

Fig.5 Configuration of the problem

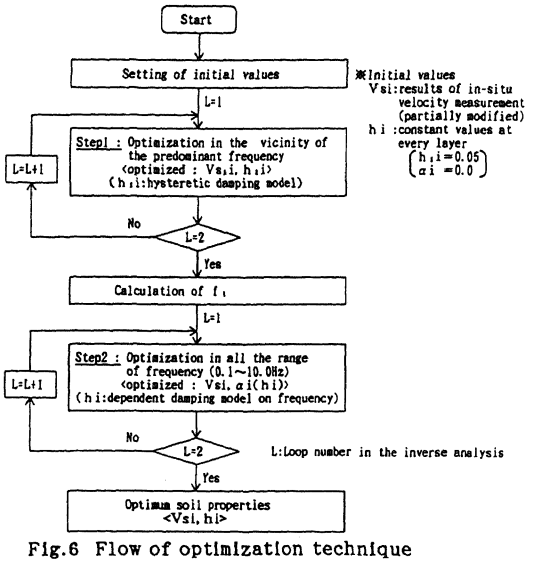

Fig.6 Flow of optimization technique

4.2 Optimum soil properties

The spectral matching was good for almost all the earthquakes at both sites. The results of the spectral matching and the optimum soil properties of each layer at the NAKA observatory in the Sendai area are shown in Fig.7 and Fig.8, respectively, as an example. It is found that the optimum shear wave velocity corresponds well with the initial value in almost all layers, while the optimum damping factor of each layer at the predominant frequency is different from the uniform initial value and also reveals a large variation (about 5 ~ 15 % average at each site) due to soil types and earthquakes.

The coefficients α_i for all the earthquakes (except No.9 earthquake) at the HAZM site are shown in Fig.9, and also the results of the coefficients α_i at each observatory are summarized in Table 3. It is found that damping characteristics of the ground surface layers reveal dependence on frequency and are close to the Maxwell visco-elastic model on the whole, as studied previously (Kinoshita,1983).

4.3 Calculation of incident SH waves

Secondly, we calculated incident SH waves ($2E_B$; in this study, multiplied by 2) underground without the influence of the subsurface structures from both the obtained optimum soil parameters and the observed SH waves, based on the Thomson-Haskell method.

We also examined the difference of the incident SH waves obtained from the observed SH waves at the surface ($2E_B$) or underground (E_B+F_B). The results show that the maximum acceleration of the incident SH waves obtained from the observed SH waves at the surface was generally larger than underground. We thought that the incident SH waves obtained from the observed SH waves at the surface contained directly shorter period components of the observed SH waves themselves due to the local influence of layers very close to the ground surface. So we adopted the incident SH waves obtained from the observed SH waves underground, i.e., at the same depth.

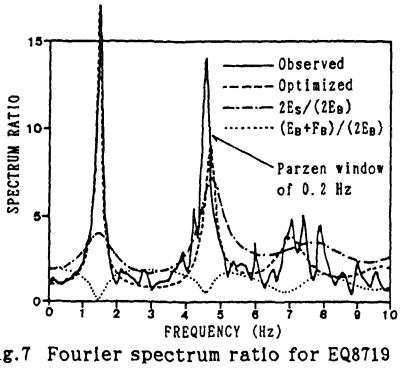

Fig.7 Fourier spectrum ratio for EQ8719 earthquake at NAKA observatory in Sendai

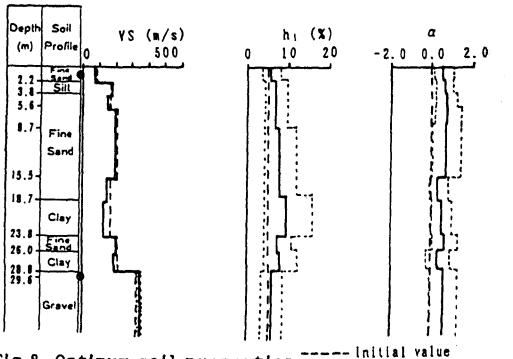

Fig.8 Optimum soil properties at NAKA observatory in Sendai

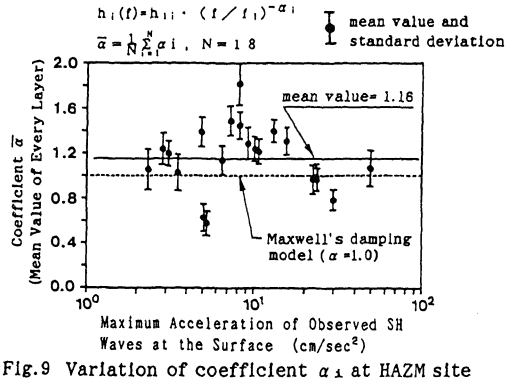

Fig.9 Variation of coefficient α_i at HAZM site

Table 3 Summary of coefficient α_i at each site

Site		HAZM	Sendai						Mean
			MIYA	NAKA	TAMA	TSUT	OKIN	TRMA	SHIR	
Number	Earthq.	21	12	11	8	5	4	6	6	
	Layer	18	6	10	3	7	7	7	6	
Mean $\bar{\alpha}$		1.16	0.50	0.59	–	1.08	(1.16)*	1.18	(0.89)*	0.94
St.dev. σ		0.28	0.10	0.13	–	0.25	–	0.37	–	

*Values in the parenthesis are because of partially insufficient spectral matching.

4.4 Response spectra

Fig.10 shows the comparison of velocity response spectra with a damping of 5 % between the observed SH waves and the incident SH wave for No.10 earthquake at the HAZM site as an example. The velocity response spectra of the incident SH waves are generally greater than those of the observed SH waves underground on the side of short period, and the difference is remarkable in the vicinity of the predominant period of the ground surface layers (0.71 second at the HAZM site).

Ratios of velocity response spectra between the observed SH waves at the surface and the incident SH waves, which may be real transfer function standing for amplification characteristics in the ground surface layers, are shown in Fig.11 (a) and (b) for the HAZM site and the Sendai area, respectively. The results reveal that the variation of the amplification ratio due to earthquakes at the HAZM site is not very large. It is also found that the amplification ratio in the Sendai area is not as large in stiff subsurface structures (see the TAMA and MIYA observatories) but it becomes generally larger and has a peak for a longer period according to the softness of the subsurface structures.

Ratios of velocity response spectra between the incident SH waves and the observed SH waves underground, which may be convenient spectra transferring from observed SH waves to incident SH waves, are shown in Fig.12 for the HAZM site. It is found that the ratio has a peak obviously in the vicinity of the predominant period of the ground surface layers.

4.5 Multiple regression analysis of spectra

Multiple regression analysis was conducted for the velocity response spectra of both estimated incident SH waves and observed SH waves separately at each site. Multiple regression formulas used here are of two types; ordinary analysis for the HAZM site and analysis with dummy variables (Kamiyama et al.,1990) for the Sendai site, as follows:

$$\log_{10}(S_V(T)) = a(T)\cdot M + b(T)\cdot \log_{10} X + c(T) \qquad (2)$$

$$\log_{10}(S_{Vi}(T)) = a(T)\cdot M + b(T)\cdot \log_{10} X_i + c_N(T) + \sum_{j=1}^{N-1} \Delta_j(T)\cdot S_{ij} \qquad (3)$$

where $S_V(T)$ is the velocity response spectrum with 5 % damping for the HAZM site and $S_{Vi}(T)$ is the same for i observatory in the Sendai area. T is period, M is magnitude of earthquake, X and X_i is hypocentral distance [km], and N is the total number of observatories (N=7 in this study). a(T),b(T),c(T) and $c_i(T)$ are partial regression coefficients ($c_i(T)$ is constant term for i observatory in the Sendai area; $c_N(T)$ for i=N), $\Delta_j(T)$ is the correction coefficient at the j-th observatory for the N-th, and S_{ij} is a dummy variable (S_{ij} = 1 for i = j, S_{ij} = 0 for i ≠ j). $\bar{c}(T)$ stands for the average coefficient of site effects in the Sendai area.

The regression coefficients of a(T),b(T),c(T),$\bar{c}$(T) and $c_i(T)$ are shown in Fig.13 (a) ~ (d). The results reveal that the difference of a(T) and b(T) between the incident SH waves and the observed SH waves can hardly be seen but c(T) and $\bar{c}(T)$ are rather different, reflecting the influence of the subsurface structures at each site.

The results of regression for (average) velocity response spectra with a hypocentral distance of 100 Km and magnitudes of 5, 6 and 7 at each site are shown in Fig.14 (a) and (b). It is found that the regressed velocity response spectra of the incident SH waves are generally greater than the observed SH waves underground, and the difference is remarkable in the vicinity of the predominant period of the ground surface layers at the HAZM site, as mentioned above. For the Sendai area, the characteristics cannot be clearly recognized because of the average but the difference is large

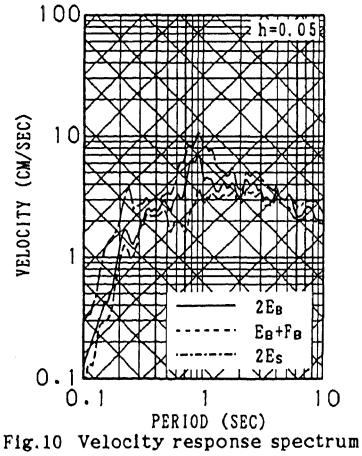

Fig.10 Velocity response spectrum for No.10 earthquake at HAZM site

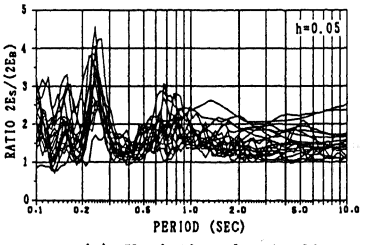

(a) Variation due to 21 earthquakes at HAZM site

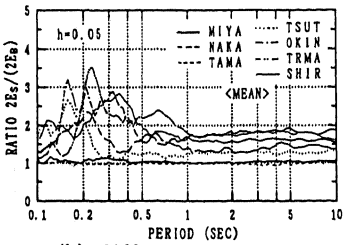

(b) Difference among 7 observatories in Sendai

Fig.11 Ratio of velocity response spectrum $2E_B/(2E_B)$

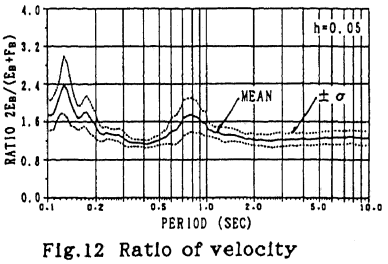

Fig.12 Ratio of velocity response spectrum $2E_B/(E_B+F_B)$ at HAZM site

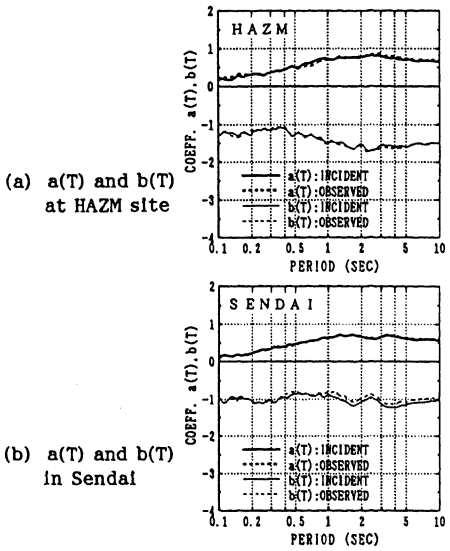

(a) a(T) and b(T) at HAZM site

(b) a(T) and b(T) in Sendai

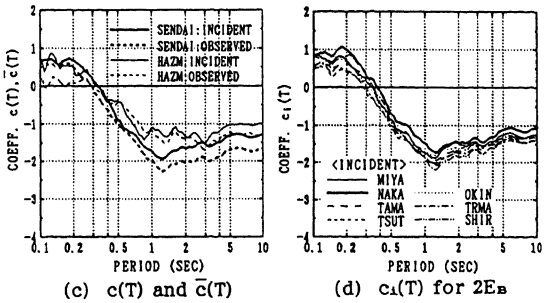

(c) c(T) and $\bar{c}$(T) at each site

(d) c_1(T) for $2E_B$ in Sendai

Fig.13 Regression coefficients of velocity response spectrum

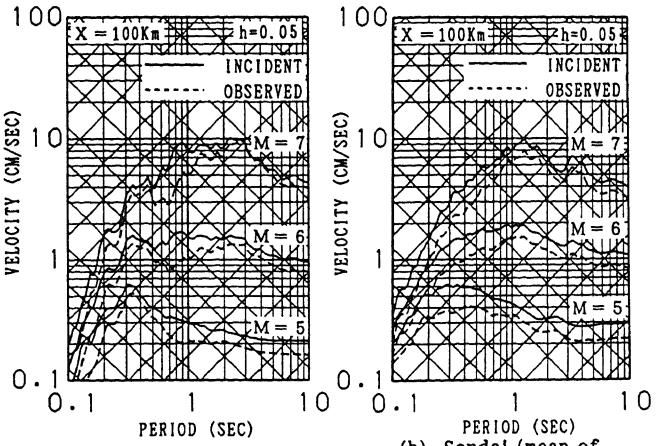

(a) HAZM site

(b) Sendai (mean of 7 observatories)

Fig.14 Results of regression for velocity response spectrum (X=100km and M=5,6,7)

in the range of short period. Finally, the spectra at both sites are almost the same size on the whole but the spectral shapes are rather different, reflecting the regional characteristics.

5 CONCLUSIONS

Soil properties of ground surface layers as well as spectral characteristics of incident SH waves penetrating into the sublayer, based on earthquake ground motion records observed at two sites in Japan, have been presented. From the analytical results, it is concluded that the damping factors of soil deposits are dependent on frequency and the velocity response spectra of the incident SH waves are generally greater than the observed SH waves underground in the range of short period, and the difference is remarkable in the vicinity of the predominant period of the ground surface layers.

ACKNOWLEDGMENTS

Some of the earthquake records used in this study have been obtained from the Dense Strong Motion Earthquake Seismometer Array Observation Project which has been implemented as a cooperative research project between the Building Research Institute (BRI), the Ministry of Construction and the Association for Promotion of Building Research. For the execution of the project, the steering committee for Dense Strong Motion Earthquake Seismometer Array Observation consisting of 18 organizations, i.e., BRI, 16 general contractors and a union of the design offices was organized by the association.

REFERENCES

Kamiyama,M. and T.Matsukawa : Attenuation analysis of strong-motion spectra with the aid of the dummy variables, Proc. of the 8th Japan Earthquake Engineering Symposium, Vol.1, pp.277-282, 1990. (In Japanese)

Kawamura,S. : Characteristics of earthquake motions observed in various kinds of ground, The 5th Symposium on Ground Vibrations, pp.45-48, 1977. (In Japanese)

Kinoshita,S. : A study for damping characteristics of surface layers, Proc. of the Japan Society of Civil Engineers, No.330, pp.15-25,1983. (In Japanese)

Kitagawa,Y., I.Ohkawa and T.Kashima : Dense strong motion earthquake seismometer array at site with different topographic and geologic conditions in Sendai, Proc. 9th WCEE, Vol.II, pp.215-220, 1988.

Kitazawa,K., S.Kawamura and Y.Osawa : An experimental study on damping characteristics of soil deposits -Shaking table test using large flexible shear vessel-, Proc. 9th WCEE, Vol.III, pp.17-22, 1988.

Sakai,S., M.Ichikawa and N.Yoshimura : Evaluation of amplification characteristics of body wave in ground surface layers, Proc. ESG (Tokyo), pp.19-24, 1989. (In Japanese)

Yokota,H. : Earthquake observations and analyses of soft soils in Tokyo, The 5th Symposium on Ground Vibrations, pp.39-44, 1977. (In Japanese)